

Hysteresis in gait transition induced by changing waist joint stiffness of a quadruped robot driven by nonlinear oscillators with phase resetting

Shinya Aoi^{1,3}, Tsuyoshi Yamashita¹, Akira Ichikawa¹, and Kazuo Tsuchiya^{2,3}

¹ Dept. of Aeronautics and Astronautics, Graduate School of Engineering, Kyoto University
Yoshida-honmachi, Sakyo-ku, Kyoto 606-8501, Japan

² Dept. of Energy and Mechanical Engineering, Faculty of Science and Engineering, Doshisha University
1-3 Tatara, Miyakodani, Kyotanabe, Kyoto 610-0394, Japan

³ JST, CREST, 5, Sanbancho, Chiyoda-ku, Tokyo 102-0075, Japan
Email: shinya_aoi@kuaero.kyoto-u.ac.jp

Abstract—In this paper, we investigated the locomotion of a quadruped robot whose front and rear bodies are connected by a roll joint. The legs of the robot are controlled by nonlinear oscillators with phase resetting. Based on numerical simulations, we showed that the robot produces various gait patterns through dynamical interactions among the robot mechanical system, oscillator control system, and environment and establishes gait transition induced by the change of the roll joint stiffness. In addition, we demonstrated that a hysteresis with respect to gait pattern occurs during the gait transition similarly to humans and animals, and we examined the mechanisms of the hysteresis from a dynamic viewpoint.

I. INTRODUCTION

Humans and animals create adaptive walking in diverse environments by cooperatively and skillfully manipulating their complicated and redundant musculoskeletal systems. They walk on level ground, up or down slopes, fast or slowly, and turn left or right. Some animals crawl, walk quadrupedally or bipedally, run, hop, leap, and jump, depending on the situation. One objective in robotics is to reproduce such locomotor behaviors and elucidate the mechanisms in motion generation and control. Furthermore, exploiting such findings in various fields is crucial, which have attracted many researchers to develop various legged robots and control systems.

As a characteristic of adaptive walking behaviors, humans and animals change their gait pattern depending on locomotion speed, e.g., walk and run for humans and walk, trot, and gallop for quadrupeds. In addition, experimental studies have shown that they normally show a hysteresis with respect to gait pattern, where the gait transition occurs at different locomotion speeds depending on the direction of speed change [9], [14], [16], [20], [25], [26], [32]. Although gait transition has been investigated from various viewpoints such as mechanics, energetics, kinematics, and kinetics [10], [15], [25], [32], the evidence concerning the determinant for the transition is still inconclusive.

In our previous works, we developed a locomotion control system for legged robots using nonlinear oscillators with phase resetting [1], [2], [30], inspired by the functional roles in central pattern generators (CPGs) that have great contribution to generating adaptive locomotion [13], [24], [27], as used to develop locomotion control systems for various

legged robots [17], [18]. Our control system generates the robot motions based on rhythm information using oscillator phases and regulates them by resetting the phases based on touch sensor signals, which modulates locomotor rhythm and phase. Numerical simulations and hardware experiments showed the effectiveness of improving robustness against disturbances and environmental variations [1], [2]. In addition, mathematical analyses based on simple walking models demonstrated the usefulness of our locomotion control system [3], [4]. Despite so simple control system that it just uses the joint angle and touch sensory information, the robots establish adaptive behavior similar to humans and animals. For example, a biped robot autonomously changes the gait cycle duration depending on the environmental situations [1] and modulates duty factors and phase relationship between the legs during turning behavior [2] as humans [8]. A quadruped robot changes the gait pattern from walk to trot depending on locomotion speed [30]. These adaptive behaviors result from dynamic interactions among the robot mechanical system, oscillator control system, and environment. Although the control system is simple, such obtained adaptabilities are notable.

In this paper, we improved the locomotion control system, and based on numerical simulations we examined dynamic characteristics of locomotion in a quadruped robot whose front and rear bodies are connected by a roll joint. We show that the robot creates various gait patterns through dynamical interactions among the robot mechanical system, oscillator control system, and environment and establishes gait transition between the walk (crawl) and trot patterns induced by the change of the roll joint stiffness, where a hysteresis appears similar to humans and animals. In addition, we investigated the mechanisms of the hysteresis from a dynamic viewpoint.

II. QUADRUPED ROBOT

Figure 1 shows a schematic model of the quadruped robot composed of two bodies and four legs. Each leg consists of two links connected by pitch joints. The bodies are connected with the other by a roll joint (waist joint). Each joint is manipulated by a motor. A touch sensor is attached to the tip of each leg.

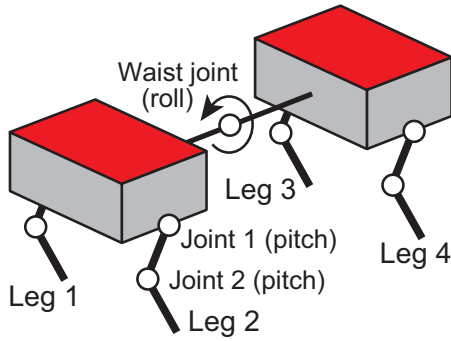


Fig. 1. Schematic model of quadruped robot

TABLE I
PHYSICAL PARAMETERS OF QUADRUPED ROBOT

Link	Parameter	Value
Body	Mass [kg]	1.0
	Length [cm]	10.0
	Width [cm]	10.0
Upper Leg	Mass [kg]	0.1
	Length [cm]	8.0
Lower Leg	Mass [kg]	0.1
	Length [cm]	8.0

The legs are enumerated from Leg 1 to 4. The leg joints are numbered Joints 1 and 2. To describe the robot configuration, we introduce angles θ_j^i ($i = 1, \dots, 4$, $j = 1, 2$) and θ_w for the rotation angles of Joint j of Leg i and waist joint, respectively.

For the numerical simulation, we derived the equation of motion of the robot model using Lagrangian equations and solved the equation of motion using the fourth order Runge-Kutta method with step size of 0.1 ms. Table I shows the physical parameters.

III. LOCOMOTION CONTROL SYSTEM

The locomotion control system consists of a motion generator and a motion controller (Fig. 2A). The motion generator is composed of a gait generator, a rhythm generator, and a trajectory generator, which generates the desired leg motions based on the desired locomotion speed and gait pattern. The gait generator creates basic gait pattern by the phase relationship between the leg movements. The rhythm generator produces basic locomotor rhythm and phase for the leg motions using four oscillators (Leg 1...4 oscillators) and touch sensory information (Fig. 2B). The trajectory generator creates the desired leg joint trajectories based on the oscillator phases. The motion controller consists of motor controllers that manipulate the joint angles by motors based on the desired trajectories.

A. Trajectory generator

In this control system, we use four oscillators (Leg 1...4 oscillators). Leg i oscillator ($i = 1, \dots, 4$) generates the desired joint motions of Leg i . First, we introduce ϕ_i ($i = 1, \dots, 4$) for the phase of Leg i oscillator.

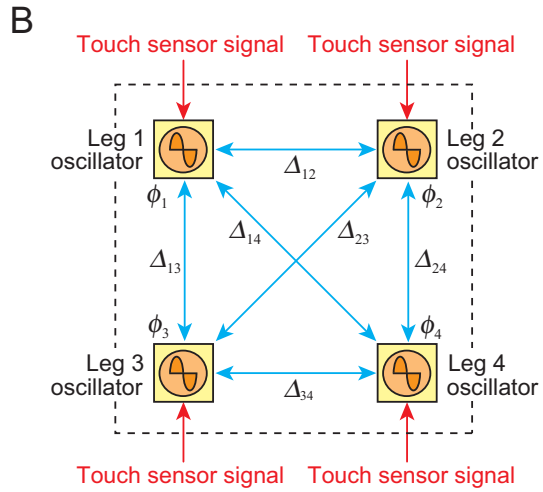
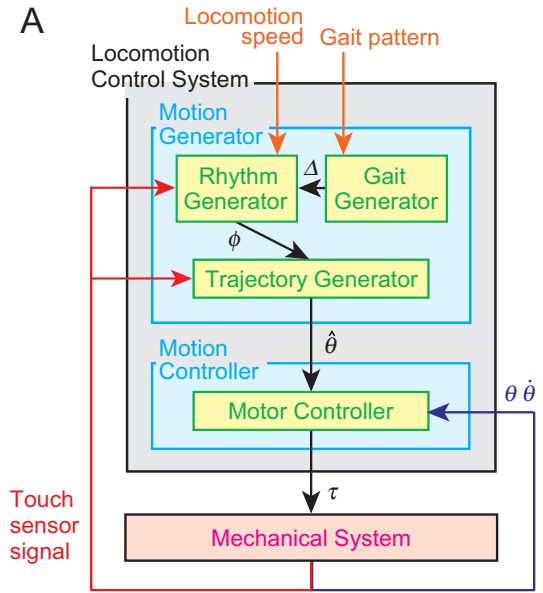


Fig. 2. Locomotion control system (A: architecture of control system, B: rhythm generator with four oscillators)

The desired motions of the leg joints are designed by the desired trajectory of the leg tip relative to the body in the pitch plane, which consists of the swing and stance phases (Fig. 3). The former is composed of a simple closed curve that includes an anterior extreme position (AEP) and a posterior extreme position (PEP). It starts from point PEP and continues until the leg tip touches the ground. The latter consists of a straight line from the landing position (LP) to point PEP, meaning that this trajectory depends on the timing of foot contact in each step cycle. Distance between points AEP and PEP is given by D . Nominal duty factor β is given by the ratio between the stance phase and step cycle durations when the leg tip touches the ground at AEP (LP = AEP). These two desired trajectories provide desired motion $\hat{\theta}_j^i$ ($i = 1, \dots, 4$, $j = 1, 2$) of Joint j of Leg i by the function of phase ϕ_i of Leg i oscillator, where we used $\phi_i = 0$ at point PEP and $\phi_i = \phi_{\text{AEP}} (= 2\pi(1 - \beta))$ at point

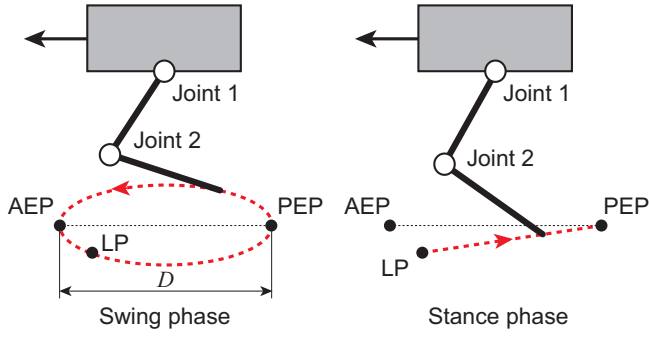


Fig. 3. Desired leg trajectories composed of swing and stance phases. When leg tip lands on ground, trajectory changes from swing to stance phase. When leg tip reaches point PEP, trajectory moves into swing phase.

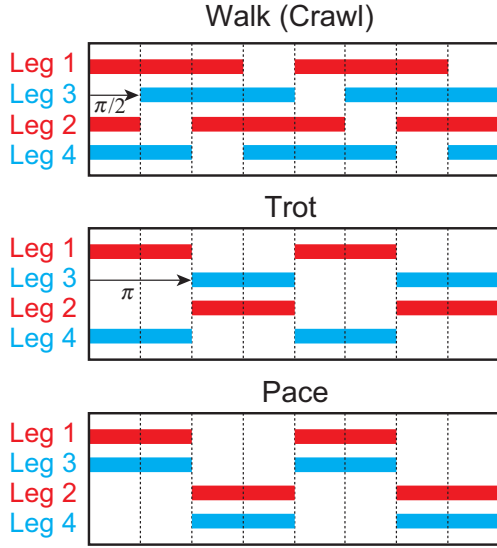


Fig. 4. Footprint diagram for walk (crawl), trot, and pace pattern, where right and left legs move out of phase in each body (forelegs in red and hindlegs in blue)

AEP.

B. Gait generator

The desired motions of the leg joints, designed by the oscillator phases, are the same among the legs. Therefore, the gait pattern is determined by the phase difference between the oscillators, which is given by matrix Δ_{ij} ($0 \leq \Delta_{ij} < 2\pi$) as follows;

$$\Delta_{ij} = \phi_i - \phi_j, \quad i, j = 1, \dots, 4 \quad (1)$$

where $\Delta_{ij} = -\Delta_{ji}$, $\Delta_{ij} = \Delta_{ik} + \Delta_{kj}$, and $\Delta_{ii} = 0$ ($i, j, k = 1, \dots, 4$) are satisfied. Therefore, the gait pattern is determined by three parameters such as $[\Delta_{12}, \Delta_{13}, \Delta_{34}]$. For example, $[\Delta_{12}, \Delta_{13}, \Delta_{34}] = [\pi, \pi/2, \pi]$ is satisfied for the walk (crawl) pattern, $[\Delta_{12}, \Delta_{13}, \Delta_{34}] = [\pi, \pi, \pi]$ is satisfied for the trot pattern, and $[\Delta_{12}, \Delta_{13}, \Delta_{34}] = [\pi, 0, \pi]$ is satisfied for the pace pattern (Fig. 4).

The gait generator produces the basic relationship between the oscillators Δ_{ij} based on the desired gait pattern.

C. Rhythm generator

The rhythm generator creates the basic rhythm for the locomotor behavior by using four oscillators (Leg 1...4 oscillators) that produce rhythmic behaviors by following phase dynamics

$$\dot{\phi}_i = \omega + g_{1i} + g_{2i}, \quad i = 1, \dots, 4 \quad (2)$$

where ω is the basic oscillator frequency that uses the same value among the oscillators, g_{1i} ($i = 1, \dots, 4$) is the function regarding the gait pattern shown below, and g_{2i} ($i = 1, \dots, 4$) is the function arising from phase resetting by touch sensor signals given below.

The locomotion speed is determined by the distance between points AEP and PEP, step cycle, and duty factor. To achieve desired locomotion speed v , swing phase duration T_{sw} is determined by

$$T_{sw} = \frac{1 - \beta}{\beta} \frac{D}{v} \quad (3)$$

In that case, oscillator frequency ω is given by

$$\omega = 2\pi \frac{1 - \beta}{T_{sw}} \quad (4)$$

Note that they are satisfied regardless of gait pattern.

1) *Gait pattern control*: Function g_{1i} in (2) manipulates the phase difference between the oscillators regarding the gait pattern, given by

$$g_{1i} = - \sum_{j=1}^4 K_{ij} \sin(\phi_i - \phi_j - \Delta_{ij}), \quad i = 1, \dots, 4 \quad (5)$$

where K_{ij} ($i, j = 1, \dots, 4$) is gain constant ($K_{ij} \geq 0$). When we use a large value for K_{ij} , $\phi_i - \phi_j = \Delta_{ij}$ will be satisfied. These interactions among the oscillators are shown by the blue arrows in Fig. 2B.

2) *Phase and rhythm modulation by phase resetting*: Functional roles of phase resetting to modulate motor commands based on sensory information in generation of adaptive walking has been investigated [6], [23] and the resetting mechanism has been used for legged robots [1], [2], [22], [23], [30]. To create adaptive locomotor behavior through dynamic interactions among the robot mechanical system, oscillator control system, and environment, we modulated the locomotor phase and rhythm by phase resetting based on touch sensor signals. Function g_{2i} in (2) corresponds to this regulation. When the tip of Leg i lands on the ground, phase ϕ_i of Leg i oscillator is reset to ϕ_{AEP} from ϕ_{land}^i at the landing ($i = 1, \dots, 4$). Therefore, functions g_{2i} is written by

$$g_{2i} = (\phi_{AEP} - \phi_{land}^i) \delta(t - t_{land}^i), \quad i = 1, \dots, 4 \quad (6)$$

where t_{land}^i is the time when the tip of Leg i touches the ground ($i = 1, 2$) and $\delta(\cdot)$ denotes Dirac's delta function. Note that touch sensor signals not only modulate the locomotion phase and rhythm but also switch the leg movements from the swing to the stance phase, as described above.

D. Motor controller

The motor controller manipulates the joint motions. For the leg joints, it produces input torque u_j^i ($i = 1, \dots, 4$, $j = 1, 2$) for Joint j of Leg i based on desired joint trajectory $\hat{\theta}_j^i$ generated by phase ϕ_i of Leg i oscillator, which is given by

$$u_j^i = -\kappa_j^i \{\theta_j^i - \hat{\theta}_j^i(\phi_i)\} - \sigma_j^i \dot{\theta}_j^i, \quad i = 1, \dots, 4, \quad j = 1, 2 \quad (7)$$

where κ_j^i and σ_j^i ($i = 1, \dots, 4$, $j = 1, 2$) are gain constants and we used adequately large value for them to achieve the desired motions. In contrast, it controls the waist joint with the desired angle maintained at zero like a spring and damper system. Therefore, input torque u_w for the waist joint is given by

$$u_w = -\kappa_w \theta_w - \sigma_w \dot{\theta}_w \quad (8)$$

where κ_w and σ_w are gain constants.

IV. NUMERICAL SIMULATION

A. Conditions for gait pattern

During the locomotion, the gait pattern is determined by the phase relationship between the oscillators, which is achieved by the interactions among the oscillators (5) and the phase regulation by phase resetting (6). When we use neither (5) nor (6), the phase relationship remains the initial state and the gait pattern never changes. When all elements of matrix Δ_{ij} are determined based on the desired gait pattern and large values are used for gain constants K_{ij} in (5), the robot will establish the desired gait pattern when the gait pattern is stable. In contrast, when small values are used for gain constants K_{ij} , the robot can produce different gait pattern from the desired due to the phase regulation by phase resetting (6).

In this paper, we focused on the gait pattern, where the right and left legs move out of phase in each body. That is, we used

$$\Delta_{12} = \Delta_{34} = \pi \quad (9)$$

and a large value for gain constants K_{12} , K_{21} , K_{34} , and K_{43} . In contrast, we used zero for the other gain constants K_{ij} , which means that the phase relationship between the forelegs and hindlegs, such as Δ_{13} , has no constraint and will be determined through locomotion dynamics. Under these conditions, the gait pattern is determined by one phase relationship, such as Δ_{13} . For example, the robot establishes the walk (crawl) pattern when $\Delta_{13} = \pi/2$, the trot pattern when $\Delta_{13} = \pi$, and the pace pattern when $\Delta_{13} = 0$ (Fig. 4).

The gait generator produces desired phase relationship (9), which means two constraints. During the locomotion in numerical simulations, the gait pattern determined by one parameter, such as Δ_{13} , will be obtained through dynamic interactions among the robot mechanical system, oscillator control system, and environment.

B. Change of waist joint stiffness

During animal locomotion, not only locomotion speed but also physical conditions such as carrying weights affect the gait transition [10]. Experimental studies in a quadruped robot demonstrated that the waist joint stiffness has much contribution to the gait transition [31]. In this paper, we focused on the examination of the roles of the waist joint stiffness in our quadruped robot model. We changed gain constants κ_w and σ_w in (8) using parameter f as follows;

$$\kappa_w = \kappa_0 (2\pi f)^2, \quad \sigma_w = 2\kappa_0 \zeta_0 (2\pi f) \quad (10)$$

where κ_0 and ζ_0 are set to 0.05 and 1.0, respectively [5].

C. Hysteresis in gait transition

To investigate the effects of the waist joint stiffness in locomotor behavior, we gradually increased or decreased parameter f in (10) during locomotion. We examined what gait pattern, represented by phase difference Δ_{13} , emerges and how the gait pattern changes through locomotion dynamics.

Figure 5 shows the result, where we used the following parameters: $D = 6.6$ cm, $\beta = 0.75$, $K_{12} = K_{21} = K_{34} = K_{43} = 10.0$, and $v = 0.22$ m/s. Figure 5A displays the phase difference between right foreleg and right hindleg Δ_{13} , plotted when the right hindleg touches the ground. Figure 5B shows the footprint diagram during the locomotion (also see the supplemental movie for the generated locomotor behaviors). When we used high joint stiffness, phase difference Δ_{13} is near $\pi/2$, implying that the walk (crawl) pattern is created. In contrast, when we used low joint stiffness, phase difference Δ_{13} is close to π , meaning that the trot pattern is produced. When the joint stiffness changes, phase difference Δ_{13} varies from $\pi/2$ to π or from π to $\pi/2$, indicating that the gait pattern changes between the walk (crawl) and trot patterns. In particular, when we increased the joint stiffness, the trot pattern changed to the walk (crawl) pattern around $f = 4.5$. On the other hand, when we decreased the joint stiffness, the walk (crawl) pattern changed to the trot pattern around $f = 2.7$. This means that the gait transition occurs at different joint stiffnesses depending on the direction of stiffness change, that is, a hysteresis with respect to gait pattern appears.

D. Stability characteristics in hysteresis

The hysteresis in gait transition obtained in the previous section suggests the coexistence of two different gait patterns over a range of the waist joint stiffness. That is, two different attractors exist in the same condition [7]. Since the gait pattern was determined by one parameter, such as Δ_{13} , as explained in Section IV-A, stability analysis related to Δ_{13} shows their existence. Therefore, to investigate the dynamic characteristics in the hysteresis, we calculated the return map of the phase difference Δ_{13} using $f = 4.0$ in (10).

Figure 6 shows the results, where we plotted the relationship between the phase difference Δ_{13n} for n th step and the phase difference Δ_{13n+5} for $n+5$ th step. This figure shows that the return map intersects with the diagonal line ($\Delta_{13n+5} = \Delta_{13n}$) at three different points. In particular,

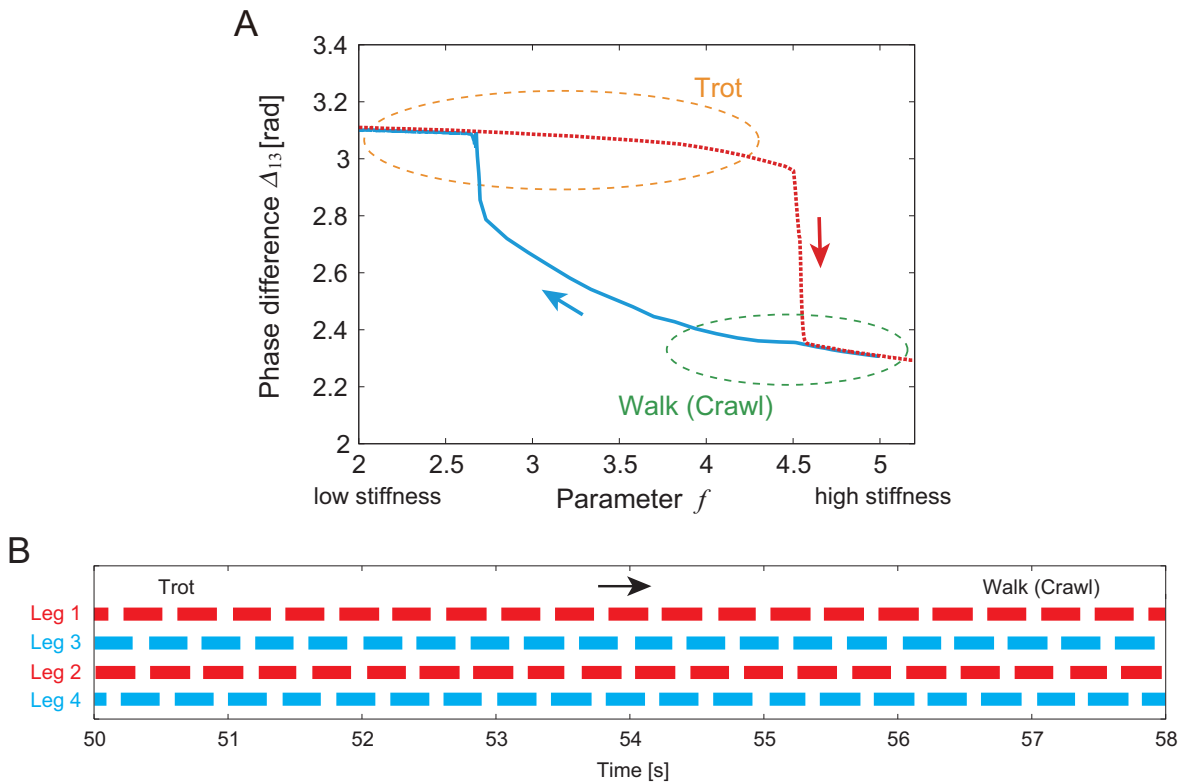


Fig. 5. Gait transition for parameter f (related to waist joint stiffness). **A** shows phase relationship between right foreleg and right hindleg Δ_{13} plotted at foot contact of right hindleg, where gait transition occurs between the walk (crawl) and trot patterns at different joint stiffnesses depending on direction of stiffness change and hysteresis appears. **B** shows footprint diagram during the gait transition from the trot to walk (crawl) pattern.

the return map intersects with the diagonal line near $\pi/2$ and π , and the slopes of the return map at the intersections near $\pi/2$ and π are 0.22 and 0.53, respectively. That is, the eigenvalues of the periodic locomotion dynamics are 0.74 near $\pi/2$ and 0.88 near π , which are less than 1 and larger than -1 . This means that there are two different attractors; one is near $\Delta_{13} = \pi/2$ and implies that stable walk (crawl) pattern exists, and the other is close to $\Delta_{13} = \pi$ and indicates that stable trot pattern also exists. These results conclude that two different attractors exist in this physical condition of the waist joint stiffness ($f = 4.0$) and the obtained hysteresis is attributed to this dynamic property.

V. CONCLUSION

In this paper, we investigated the locomotion of a quadruped robot driven by nonlinear oscillators with phase resetting based on numerical simulations. We showed that it changes the gait pattern depending on the waist joint stiffness and shows a hysteresis with respect to gait pattern during the gait transition similar to humans and animals despite so simple and different mechanical and control systems. Many simulation studies for the locomotion of humans and animals have demonstrated that a hysteresis occurs during the gait transition through dynamic interactions among the musculoskeletal system, nervous system, and environment [19], [28], [29]. The investigation of hysteresis is expected to provide the clues to clarify the mechanisms in motion generation and control strategy.

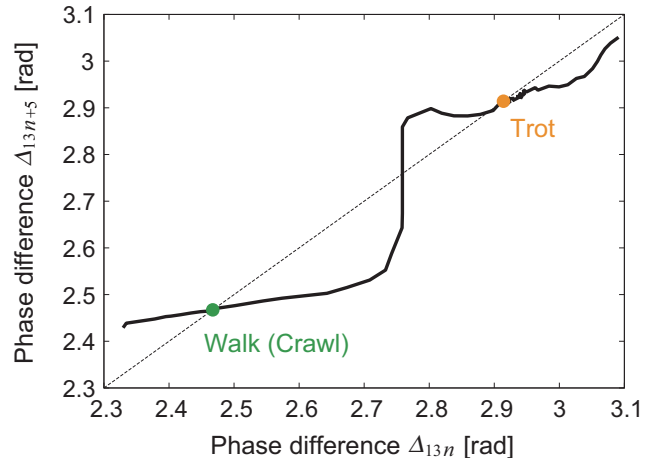


Fig. 6. Return map of phase difference Δ_{13} with $f = 4.0$

In robotics, the changes in gait patterns induced by the changes in physical conditions have also been investigated using various legged robots. For example, the walking behavior of passive dynamic walking [21] leads to a chaotic motion through consecutive period-doubling bifurcations as the slope angle increases, calculated based on the simple mathematical model [11], [12]. The gait of a multilegged modular robot, whose bodies are connected by yaw joints, changes from straight to meandering walk through Hopf

bifurcation by changing the yaw joint stiffness [5]. In contrast to humans and animals, a hysteresis does not appear during these gait transitions of the robot systems. It is because different attractors corresponding to gait patterns do not exist in the same condition and only one gait pattern is stable.

The hysteresis with respect to gait pattern obtained in this paper was produced through dynamical interactions among the robot mechanical system, oscillator control system, and environment. A hysteresis is a typical characteristic for non-linear dynamical systems. Toward understanding the transition mechanisms in locomotion dynamics, the mathematical modeling to explain the essence and the verification using hardware experiments in the real world should be conducted in future studies.

ACKNOWLEDGMENTS

This paper is supported in part by a Grant-in-Aid for Creative Scientific Research (No. 19GS0208) from the Japanese Ministry of Education, Culture, Sports, Science and Technology.

REFERENCES

- [1] S. Aoi and K. Tsuchiya, *Locomotion control of a biped robot using nonlinear oscillators*, *Auton. Robots*, 19(3): 219–232, 2005.
- [2] S. Aoi and K. Tsuchiya, *Adaptive behavior in turning of an oscillator-driven biped robot*, *Auton. Robots*, 23(1): 37–57, 2007.
- [3] S. Aoi and K. Tsuchiya, *Stability analysis of a simple walking model driven by an oscillator with a phase reset using sensory feedback*, *IEEE Trans. Robotics*, 22(2):391–397, 2006.
- [4] S. Aoi and K. Tsuchiya, *Self-stability of a simple walking model driven by a rhythmic signal*, *Nonlinear Dyn.*, 48(1-2):1–16, 2007.
- [5] S. Aoi, H. Sasaki, and K. Tsuchiya, *A multilegged modular robot that meanders: Investigation of turning maneuvers using its inherent dynamic characteristics*, *SIAM J. Appl. Dyn. Syst.*, 6(2):348–377, 2007.
- [6] S. Aoi, N. Ogihara, T. Funato, Y. Sugimoto, and K. Tsuchiya, *Evaluating functional roles of phase resetting in generation of adaptive human bipedal walking with a physiologically based model of the spinal pattern generator*, *Biol. Cybern.*, 102(5):373–387, 2010.
- [7] C.C. Canavier, R.J. Butera, R.O. Dror, D.A. Baxter, J.W. Clark, and J.H. Byrne, *Phase response characteristics of model neurons determine which patterns are expressed in a ring circuit model of gait generation*, *Biol. Cybern.*, 77:367–380, 1997.
- [8] G. Courtine and M. Schieppati, *Human walking along a curved path. II. Gait features and EMG patterns*, *Eur. J. Neurosci.*:18(1):191–205, 2003.
- [9] F.J. Diedrich and W.H. Warren, *Why change gaits? Dynamics of the walk-run transition*, *J. Exp. Psychol. Hum. Percept. Perform.*, 21:183–202, 1998.
- [10] C.T. Farley and C.R. Taylor, *A mechanical trigger for the trot-gallop transition in horses*, *Science*, 253:306–308, 1991.
- [11] M. Garcia, A. Chatterjee, A. Ruina, and M. Coleman, *The simplest walking model: stability, complexity, and scaling*, *ASME J. Biomech. Eng.*, 120(2):281–288, 1998.
- [12] A. Goswami, B. Thuilot, and B. Espiau, *A study of the passive gait of a compass-like biped robot: symmetry and chaos*, *Int. J. Robot. Res.*, 17(12):1282–1301, 1998.
- [13] S. Grillner, *Locomotion in vertebrates: central mechanisms and reflex interaction*, *Physiol. Rev.*, 55(2):247–304, 1975.
- [14] N.C. Heglund and C.R. Taylor, *Speed, stride frequency and energy cost per stride: how do they change with body size and gait?*, *J. Exp. Biol.*, 138:301–318, 1998.
- [15] D.F. Hoyt and C.R. Taylor, *Gait and the energetics of locomotion in horses*, *Nature*, 292:239–240, 1981.
- [16] A. Hreljac, R. Imamura, R.F. Escamilla, and W.B. Edwards, *Effects of changing protocol, grade, and direction on the preferred gait transition speed during human locomotion*, *Gait Posture*, 25:419–424, 2007.
- [17] A.J. Ijspeert, *Central pattern generators for locomotion control in animals and robots: a review*, *Neural Netw.*, 21(4):642–653, 2008.
- [18] H. Kimura, Y. Fukuoka, and A. Cohen, *Adaptive dynamic walking of a quadruped robot on natural ground based on biological concepts*, *Int. J. Robotics Res.*, 26(5):475–490, 2007.
- [19] S. Kimura, M. Yano, and H. Shimizu, *A self-organizing model of walking patterns of insects*, *Biol. Cybern.*, 69:183–193, 1993.
- [20] C.J.C. Lamoth, A. Daffertshofer, R. Huys, and P.J. Beek, *Steady and transient coordination structures of walking and running*, *Hum. Mov. Sci.*, 28:371–386, 2009.
- [21] T. McGeer, *Passive dynamic walking*, *Int. J. Robot. Res.*, 9(2):62–82, 1990.
- [22] J. Nakanishi, J. Morimoto, G. Endo, G. Cheng, S. Schaal, and M. Kawato, *Learning from demonstration and adaptation of biped locomotion*, *Robot. Auton. Syst.*, 47(2-3):79–91, 2004.
- [23] T. Nomura, K. Kawa, Y. Suzuki, M. Nakanishi, and T. Yamasaki, *Dynamic stability and phase resetting during biped gait*, *Chaos*, 19:026103, 2009.
- [24] G.N. Orlovsky, T. Deliagina, and S. Grillner, *Neuronal control of locomotion: from mollusc to man*, *Oxford University Press*, 1999.
- [25] A.J. Raynor, C.J. Yi, B. Abernethy, and Q.J. Jong, *Are transitions in human gait determined by mechanical, kinetic or energetic factors?*, *Hum. Mov. Sci.*, 21:785–805, 2002.
- [26] V. Segers, P. Aerts, M. Lenoir, and D.De Clercq, *Spatiotemporal characteristics of the walk-to-run and run-to-walk transition when gradually changing speed*, *Gait Posture*, 24:247–254, 2006.
- [27] M.L. Shik and G.N. Orlovsky, *Neurophysiology of locomotor automatism*, *Physiol. Rev.*, 56(3):465–501, 1976.
- [28] G. Taga, Y. Yamaguchi, and H. Shimizu, *Self-organized control of bipedal locomotion by neural oscillators in unpredictable environment*, *Biol. Cybern.*, 65: 147–159, 1991.
- [29] G. Taga, *A model of the neuro-musculo-skeletal system for human locomotion II. - Real-time adaptability under various constraints*, *Biol. Cybern.*, 73: 113–121, 1995.
- [30] K. Tsujita, K. Tsuchiya, and A. Onat, *Adaptive gait pattern control of a quadruped locomotion robot*, *Proc. IEEE/RSJ Int. Conf. on Intell. Robots Syst.*, pp. 2318–2325, 2001.
- [31] K. Tsujita, T. Kobayashi, T. Inoura, and T. Masuda, *Gait transition by tuning muscle tones using pneumatic actuators in quadruped locomotion*, *Proc. IEEE/RSJ Int. Conf. on Intell. Robots Syst.*, pp. 2453–2458, 2008.
- [32] M.T. Turvey, K.G. Holt, M.E. LaFlandra, and S.T. Fonseca, *Can the transition to and from running and the metabolic cost of running be determined from the kinetic energy of running?*, *J. Mot. Behav.*, 31:265–278, 1999.